Max-Planck-Institut für Mathematik in den Naturwissenschaften Leipzig

Black-Box Hartree-Fock Solver by the Tensor Numerical Methods

(revised version: October 2013)

by

Venera Khoromskaia

Preprint no.: 90 2013

Black-Box Hartree-Fock Solver by the Tensor Numerical Methods

V. KHOROMSKAIA*

Abstract

The Hartree-Fock eigenvalue problem governed by the 3D integro-differential operator is the basic model in *ab initio* electronic structure calculations. Several years ago the idea to solve the Hartree-Fock equation by fully 3D grid based numerical approach seemed to be a fantasy, and the tensor-structured methods did not exist. In fact, these methods evolved during the work on this challenging problem. In this paper, our recent results on the topic are outlined and the black-box Hartee-Fock solver by the tensor numerical methods is presented. The approach is based on the rank-structured calculation of the core hamiltonian and of the two-electron integrals tensor using the problem adapted basis functions discretized on $n \times n \times n$ 3D Cartesian grids. The arising 3D convolution transforms with the Newton kernel are replaced by a combination of 1D convolutions and $1D$ Hadamard and scalar products. The approach allows huge spatial grids, with $n^3 \simeq 10^{15}$, yielding high resolution at low cost. The two-electron integrals are computed via multiple factorizations. The Laplacian Galerkin matrix can be computed "on-the-fly" using the quantized tensor approximation of $O(\log n)$ complexity. The performance of the black-box solver in Matlab implementation is compatible with the benchmark packages based on the analytical (pre)evaluation of the multidimensional convolution integrals. We present *ab initio* Hartree-Fock calculations of the ground state energy for the amino acid molecules, and of the "energy bands" for the model examples of extended (quasi-periodic) systems.

AMS Subject Classification: 65F30, 65F50, 65N35, 65F10
*Key words:*Hartree-Fock equation, Hartree-Fock solver, tensor-structured numerical methods, Fock operator, 3D grid-based tensor approximation, two-electron integrals, core Hamiltonian, quantized tensor approximation.

1 Introduction

The Hartree-Fock (HF) equation governed by the 3D integro-differential operator is the basic model in *ab initio* calculations of the ground state energy and electronic structure of molecular systems [43, 12]. Only several years ago the idea to solve this problem using a 3D grid-based fully discrete numerical method seemed to be a fantasy.

*Max-Planck-Institute for Mathematics in the Sciences, Inselstr. 22-26, D-04103 Leipzig, Germany (vekh@mis.mpg.de).

Why is the Hartree-Fock problem so difficult? First, it is a nonlinear eigenvalue problem (EVP) in a sense, that one should find the solution to the problem when the part of the governing operator depends on the eigenvectors. This dependence is expressed by the convolution of the electron density, which is a function of the solution, with the Newton kernel in $\mathbb{R}^3$. Also, multiple strong singularities due to nuclear cusps in the electron density of a molecule impose strong requirements on the accuracy of HF calculations. Finally, the eigenvalues and the ground state energy should be computed with high accuracy to be suitable for more precise post-Hartree-Fock computations. Thus, the standard numerical approaches with the grid refinement are not tractable owing to multiple cusps in the electron density, and because of the cubic scaling of the numerical cost with respect to the grid size.

Beginning from the 80-s, chemists developed efficient schemes for the solution of the Hartree-Fock equation using the analytical calculation of the arising 3D convolution type integrals, the so-called two-electron integrals (TEI), in the problem adapted naturally separable Gaussian-type bases [2]. Then the HF problem is solved by self-consistent field iteration (SCF), using abundance of precomputed data sets, individually adapted for every molecule [43, 12]. This rigorous approach led to a number of efficient programm packages which required years of development by large scientific groups.

This traditional approach is limited by the choice of the basis in the form of Gaussians, to enable analytical evaluation of the convolutions with the Newton kernel in $\mathbb{R}^3$ using *erf* functions. For molecules with larger atomic numbers, the approximating Gaussians become sharp, leading to a large condition number of the Galerkin matrix of the EVP. The numerical treatment of large molecular systems with heavier atoms is still a hard problem.

The idea to replace or assist the analytical computations for the HF problem by a data-sparse grid-based approach is not new. In particular, the wavelet multiresolution schemes [11], as well as the sparse grids approach in [49, 17] have been proposed. The entirely wavelet-based method is successful only for small atomic systems with one or two electrons [4]. The grid-based numerical method for the HF problem for diatomic molecules proposed in [42] is not extendable to compact (3D) molecules. The domain decomposion approach to problems with "linear geometry" of molecules is discussed in [5]. Important results on the regularity properties of the wave functions in the Schrödinger equation which forecast the possibility to reduce the computational complexity in electronic structure calculations, and motivate the data-sparse approaches to the problem have been presented in [48, 49].

The tensor-structured numerical methods, both the name and the concept, appeared during the work on the 3D grid-based tensor approach to the solution of the Hartree-Fock problem. In particular, the opportunity to verify the results of the 3D grid-based tensor approach by comparison with the 3D calculations by analytical methods of high accuracy using a standard package [44] helped to convince the scientific community [23, 21].

Apparently, the tensor numerical methods have begun in 2006, when it was proved in [32] that for a class of function related tensors the Tucker-type[1] approximation converges exponentially with respect to the Tucker rank. This gives an opportunity to represent a discretized multidimensional function (function related tensor) in an algebraically separable

[1]The Tucker tensor decomposition is since long known in the computer science community, used for example, for finding the amount of correlation in experimental data in chemometrics. The exceptional approximating properties of the Tucker decomposition for function related tensors are revealed in [32, 33], promoting its usage as a tool for the treatment of multidimensional problems in numerical analysis.

form. The canonical-to-Tucker algorithm introduced in [23, 33], for efficient canonical rank reduction of function related tensors, is a necessary tool in tensor-structured calculations. These algorithms and approximations, as well as the tensor-product convolution developed in [29], enable tractable numerical treatment of the multivariate functions and operators [23]. The important ingredient of the multidimensional tensor product convolution is the canonical tensor approximation to the Newton kernel introduced in [14, 15, 6]. Thus, it became possible to avoid the cubic scaling of computational work in the numerical treatment of functions and operators in $3D$ problems. The tensor-structured numerical methods for the 3D grid-based calculation of the Coulomb and exchange integral operators have been introduced in [23, 21, 22], when it was shown that the 3D convolution integration can be reduced to tensor calculus based on combinations of 1D convolutions, and 1D Hadamard and scalar products.

The first "Multilevel Hartree-Fock Solver" by the tensor-structured numerical methods based on above results was issued in [22, 24]. Using the discretization of the Galerkin basis on $n\times n\times n$ ($n^{\otimes 3}$) $3D$ Cartesian grids, it employs a "nonstandard" computational scheme, which does not require the precomputed TEI. Instead, the $3D$ convolution integrals (the Coulomb and exchange operators) are evaluated "on-the-fly" by *recalculating* (updating) them in $1D$ complexity at every iteration step on a sequence of refined $n^{\otimes 3}$ grids. The accuracy of the rank-structured calculations, governed by the ε-ranks of the involved tensors is estimated as $O(h^2)$, where h is the step-size of the uniform mesh. This solver, implemented in Matlab and operating on large 3D grids up to $n^3 = 16384^3$ provides good results[2] for moderate compact molecules, like H_2O, CH_4, C_2H_5OH [22].

The tensor-structured approach for the Hartree-Fock problem rests on the grid-based representation of the Galerkin basis. The "global" Galerkin basis functions are represented on a tensor grid by the piece-wise constant "local" finite elements for convolution integrals and by the piece-wise linear "local" elements for the Laplace operator. Due to substitution of the multidimensional integration by the algebraic 1D operations the choice of the Galerkin basis is not limited to functions with analytic integrability.

Due to Matlab time consumption for loops in the exchange operator, time performance of the multilevel tensor-based HF Solver is not compatible with the traditional packages. However, it was the first step in the development of tensor numerical methods, and a "proof of concept" for their applicability in electronic structure calculations. Besides, these results promoted spreading and further evolution of the tensor-structured methods in the community of numerical analysis [10, 38, 7, 34, 31, 3, 36, 28, 8, 16].

Here, we present the (second) "Black-box Hartee-Fock Solver" by the tensor numerical methods which is now compatible in performance with the traditional packages. It follows the conventional HF computational scheme as in the analytical approach (first compute TEI, then iteration runs without numerical integrations), but in a "black box" way: just specify the coordinates of nuclei of the molecule in a computational box, set the discretized Galerkin basis using $n^{\otimes 3}$ 3D Cartesian grids and run the program. But there is a big difference from the analytical approach – all calculations are 3D grid-based: evaluation of TEI, and of

[2] In $3D$ tensor-structured calculations both storage and time scale linearly in $1D$ size, while the problem is solved in the volume with the mesh size (and accuracy) corresponding to the grid with n^3 entries. The redundancy of the computer representation of the multidimensional functions and operators is avoided due to the optimized low rank approximation.

the core Hamiltonian are performed using the simple grid-based representation of the basis functions. There is no restriction that basis functions should provide analytic integrability.

In this framework, our results on fully 3D grid-based tensor-structured calculation of factorized TEI tensor and of the core Hamiltonian are applied [25, 27, 26]. Additionally, for the core Hamiltonian, we employ the quantized tensor approximation of $O(\log n)$ complexity [30, 31]. For example, the machine accuracy of the Galerkin matrix of the Laplacian for the water molecule (compared with analytical calculations) is achieved using fine grids with $n^3 \simeq 10^{18}$ entries, in two minutes in Matlab. The routine size of the 3D grid for TEI calculations in Matlab on a terminal is of the order of $n^3 \simeq 10^{14}$ (with $n = 32768$), yielding fine mesh resolution of the order of $h \simeq 10^{-4}$ $\overset{\circ}{A}$.

The performance of our black-box solver in Matlab implementation is compatible with the benchmark quantum chemical packages both in computation time and accuracy. Ab initio HF calculations for large compact molecules, up to amino acids glycine ($C_2H_5NO_2$) and alanine ($C_3H_7NO_2$), can run on a laptop. For small molecules there is no need of the precomputed data, the HF calculations can be done completely "on-the-fly": core Hamiltonian, TEI and SCF iteration for the nonlinear EVP, altogether take few minutes on a laptop.

The discretized Gaussians are still used as the Galerkin basis, due to simplicity of comparison with the Molpro calculations. Development and testing of the optimized general type bases will be considered in a separate paper. A potential advantage could be the substitution of the set of steepest core electron Gaussians by a Slater-type functions for every nonhydrogen nuclei, essentially reducing the number of "global" basis functions.

The rest of the paper is organized as follows. In §2 we discuss the formulation of the Hartree-Fock problem and the standard Galerkin scheme for its solution. In §3.1 we show the discretization of the global Galerkin basis. The tensor-structured method for the 3D Laplacian in $O(\log n)$ as well as in $O(\log n)$ complexity is considered in §3.2 and §3.3, respectively. The tensor method for the nuclear potential operator is shown in §3.4. In §3.5 we recall the tensor-structured method for calculating the two-electron integrals matrix (tensor) in a factorized form introduced in [25, 27]. The structure of the black-box algorithm is decribed in §3.6. The numerical results including the calculations of the ground state energy for the glycine and alanine amino acids and calculation of the "energy bands" for the model quasi-periodic extended molecular systems are presented in §4. In Appendix A we briefly recall that the Hartree-Fock model originates from the electronic Schrödinger equation. Appendix B presents basic rank-structured tensor formats and operations.

2 The Hartree-Fock equation

The Hartree-Fock model is a well-established procedure for finding the ground state energy of a molecular system (see Appendix A). Here we consider this problem for the closed shell systems, where the number of molecular orbitals equals to the number of electron pairs, $N_{orb} = N/2$. The Hartree-Fock equation is a nonlinear eigenvalue problem (EVP),

$$\mathcal{F}\varphi_i(x) = \lambda_i \varphi_i(x), \quad x \in \mathbb{R}^3, \tag{2.1}$$

with respect to the (orthogonal) molecular orbitals $\varphi_i(x)$,

$$\int_{\mathbb{R}^3} \varphi_i \varphi_j = \delta_{ij}, \ i = 1, ..., N_{orb}, \quad x \in \mathbb{R}^3,$$

and the Fock operator is given by

$$\mathcal{F} = H_c + V_H - \mathcal{K}. \tag{2.2}$$

The core Hamiltonian part H_c of the Fock operator consists of the kinetic energy of electrons and the nuclear potential,

$$H_c(x) = -\frac{1}{2}\Delta - \sum_{\nu=1}^{M} \frac{Z_\nu}{\|x - a_\nu\|}, \quad Z_\nu > 0, \;\; x, a_\nu \in \mathbb{R}^3. \tag{2.3}$$

Since electron correlation parts of the Fock operator, the Hartree potential,

$$V_H(x) := \int_{\mathbb{R}^3} \frac{\rho(y)}{\|x - y\|}\, dy, \quad \rho(y) = 2\sum_{i=1}^{N_{orb}} (\varphi_i(y))^2, \quad x \in \mathbb{R}^3$$

and the exchange operator

$$(\mathcal{K}\varphi)(x) := \int_{\mathbb{R}^3} \frac{\tau(x,y)}{\|x - y\|}\, \varphi(y) dy, \quad \tau(x,y) = \sum_{i=1}^{N_{orb}} \varphi_i(x)\varphi_i(y), \quad x \in \mathbb{R}^3$$

both depend on the solution of the EVP (2.1), the (nonlinear) Hartree-Fock equation is solved iteratively, by self-consistent field (SCF) iteration [43, 12]. The Hartree-Fock model is often called a mean-field approximation, in a sense that the energy of every electron in a molecule is computed with respect to the mean field created by all electrons in a molecular system, including this electron as well.

The standard Galerkin approach for the numerical solution is based on the expansion of the molecular orbitals in a Gaussian-type basis, $\{g_\mu\}_{1 \le \mu \le N_b}$,

$$\varphi_i(x) = \sum_{\mu=1}^{N_b} c_{i\mu} g_\mu(x), \quad i = 1, ..., N_{orb}, \quad x \in \mathbb{R}^3 \tag{2.4}$$

which yields the Galerkin system of nonlinear equations for the coefficients matrix $C = \{c_{i\mu}\} \in \mathbb{R}^{N_{orb} \times N_b}$, (and the density matrix $D = 2CC^* \in \mathbb{R}^{N_b \times N_b}$)

$$F(C)C = SC\Lambda, \quad \Lambda = diag(\lambda_1, ..., \lambda_{N_b}), \quad C^T S C = I_{N_b} \tag{2.5}$$

where S is the overlap matrix for the chosen Galerkin basis. The Galerkin counterpart of the Fock operator,

$$F(C) = H + J(C) + K(C), \quad H = A_g + V_g. \tag{2.6}$$

and includes the parts $A_g + V_g$ corresponding to the core Hamiltonian H_c, and $J(C)$, $K(C)$, corresponding to the operators V_H, $\mathcal{K}$, respectively. The one-electron integrals in $H = \{h_{\mu\nu}\}_{\mu,\nu=1}^{N_b}$,

$$h_{\mu\nu} = \frac{1}{2}\int_{\mathbb{R}^3} \nabla g_\mu \cdot \nabla g_\nu dx + \int_{\mathbb{R}^3} V_c(x) g_\mu g_\nu dx \quad 1 \le \mu, \nu \le N_b, \tag{2.7}$$

and the so-called two-electron integrals tensor (TEI),

$$b_{\mu\nu\kappa\lambda} = \int_{\mathbb{R}^3}\int_{\mathbb{R}^3} \frac{g_\mu(x) g_\nu(x) g_\kappa(y) g_\lambda(y)}{\|x - y\|} dxdy, \quad 1 \le \mu, \nu \le N_b, \quad x, y \in \mathbb{R}^3, \tag{2.8}$$

depend only on choice of the basis functions (2.4) and therefore may be precomputed. The solution is sought by SCF iteration, using the core Hamiltonian as the initial guess, by updating the Coulomb

$$J(C)_{\mu\nu} = \sum_{\kappa,\lambda=1}^{N_b} b_{\mu\nu,\kappa\lambda} D_{\kappa\lambda}, \tag{2.9}$$

and exchange Galerkin matrices

$$K(C)_{\mu\nu} = -\frac{1}{2} \sum_{\kappa,\lambda=1}^{N_b} b_{\mu\lambda,\nu\kappa} D_{\kappa\lambda}, \tag{2.10}$$

at every iteration step. The standard DIIS scheme introduced in [39] is used to provide the convergence of the algorithm. DIIS is based on defining the weights of the previous solutions, to be used as the initial guess for the current step of iteration.

Then the total energy is computed as

$$E_{HF} = 2 \sum_{i=1}^{N_{orb}} \lambda_i - \sum_{i=1}^{N_{orb}} \left(\widetilde{J}_i - \widetilde{K}_i \right),$$

where $\widetilde{J}_i = (\varphi_i, V_H \varphi_i)_{L^2} = \langle C_i, JC_i \rangle$ and $\widetilde{K}_i = (\varphi_i, K\varphi_i)_{L^2} = \langle C_i, KC_i \rangle$, $i = 1, ..., N_{orb}$, are the Coulomb and exchange integrals in the basis of orbitals φ_i.

The resulting ground state energy of the molecule for the given geometry of nuclei, includes the nuclear shift E_{nuc},

$$E_0 = E_{HF} + E_{nuc}, \tag{2.11}$$

where

$$E_{nuc} = \sum_{k=1}^{M} \sum_{m<k}^{M} \frac{Z_k Z_m}{\|x_k - x_m\|} \tag{2.12}$$

is the nuclei repulsion energy.

The above scheme is a well established standart for the *ab initio* Hartree-Fock calculations. In the traditional packages in quantum chemistry both the core Hamiltonian, and the two-electron integrals (2.8) are precomputed analytically in the separable Gaussian-type basis $\{g_\mu\}_{\mu=1}^{N_b} \in \mathbb{R}^3$.

3 Tensor-structured calculation of the Fock operator.

3.1 Grid representation of the basis

For the tensor-structured calculations using 3D Cartesian grids, the initial EVP is posed in the finite volume box $\Omega = [-b, b]^3 \in \mathbb{R}^3$, subject to the homogeneous Dirichlet boundary conditions on $\partial\Omega$. For a given discretization parameter $n \in \mathbb{N}$, we use the equidistant $n \times n \times n$ tensor grid $\omega_{\mathbf{3},n} = \{x_{\mathbf{i}}\}$, $\mathbf{i} \in \mathcal{I} := \{1, ..., n\}^3$, with the mesh-size $h = 2b/(n+1)$. For the set of "global" separable Galerkin basis functions $\{g_k\}_{1 \le k \le N_b}$, $k = 1, 2, \ldots N_b$, we define a set of approximating functions $\overline{g}_k := \mathbf{I}_1 g_k$, $k = 1, ..., N_b$, by linear tensor-product interpolation via

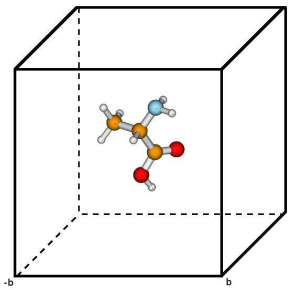

Figure 3.1: The computational box $[-b,b]^3$, routine size is $b = 20$ au (~ 10.5 $\mathring{A}$).

the set of product "local" basis functions, $\{\xi_{\mathbf{i}}\} = \xi_{i_1}(x_1)\xi_{i_2}(x_2)\xi_{i_3}(x_3)$, $\mathbf{i} \in \mathcal{I}$, associated with the respective grid-cells in $\omega_{\mathbf{3},n}$. The local basis functions are chosen piecewise linear (hat functions) for the Laplace calculations, or piece-wise constant for calculations of TEI and the nuclear potential V_c. The linear interpolant $\mathbf{I}_1 = \mathrm{I}_1 \times \mathrm{I}_1 \times \mathrm{I}_1$ is a product of 1D interpolation operators, $\overline{g}_k^{(\ell)} = \mathrm{I}_1 g_k^{(\ell)}$, $\ell = 1, 2, 3$, where $\mathrm{I}_1 : C^0([-b,b]) \to W_h := span\{\xi_i\}_{i=1}^n$ is defined over the set of (piecewise linear or piece-wise constant) local basis functions by $(\mathrm{I}_1\, w)(x_\ell) := \sum_{i=1}^N w(x_{\ell,i})\xi_i(x_\ell)$, $x_{\mathbf{i}} \in \omega_{\mathbf{3},N}$. This leads to the separable grid-based approximation of the initial basis functions $g_k(x)$,

$$g_k(x) \approx \overline{g}_k(x) = \prod_{\ell=1}^{3} \overline{g}_k^{(\ell)}(x_\ell) = \prod_{\ell=1}^{3} \sum_{i=1}^{N} g_k^{(\ell)}(x_{\ell,i})\xi_i(x_\ell), \tag{3.1}$$

where the rank-1 coefficients tensor $\mathbf{G}_k$ is given by

$$\mathbf{G}_k = G_k^{(1)} \otimes G_k^{(2)} \otimes G_k^{(3)}, \tag{3.2}$$

with the canonical vectors $G_k^{(\ell)} = \{g_{k_i}^{(\ell)}\} \equiv \{g_k^{(\ell)}(x_i^{(\ell)})\}$. The discretized Galerkin basis is then presented in the canonical tensor format,

$$\mathbf{G} = \sum_{k=1}^{N_b} \mathbf{G}_k = \sum_{k=1}^{N_b} G_k^{(1)} \otimes G_k^{(2)} \otimes G_k^{(3)}. \tag{3.3}$$

Since the tensor-structured calculation of the operators in the HF EVP is reduced to 1D rank-structured algebraic operations, the size n of the tensor-product grid $\omega_{\mathbf{3},n}$ can be chosen different for separate parts of the Fock operator. For example, the entries of the matrices in A_g and V_g in (2.6) corresponding to kinetic and nuclear energy parts, can be computed using different grid sizes n for discretizing the "global" basis functions. The same for the grid size n in tensor calculation of TEI, which can be much smaller than n for both A_g and V_g, since J and K are the integral operators. Thus, the discretization step-size for the EVP Galerkin basis is defined only by accuracy needs for the given part of the Fock operator.

The Galerkin tensor representation of the identity operator leads to the following mass matrix, $S = \{\overline{s}_{km}\}$,

$$\overline{s}_{km} = \int_{\mathbb{R}^3} \overline{g}_k(x)\overline{g}_m(x)dx \approx \langle \mathbf{G}_k, \mathbf{G}_m \rangle, \quad 1 \le k, m \le N_b.$$

Next, we present the grid-based calculation of the core Hamiltonian part (2.2),

$$H_c = -\frac{1}{2}\Delta_{(3)} + V_c,$$

with respect to the discretized Galerkin basis (3.3).

3.2 3D Laplace operator in 1D complexity

Applied to a separable continuous function $g(x) = g(x_1)g(x_2)g(x_3)$, $x = (x_1, x_2, x_3) \in \mathbb{R}^3$, the Laplace operator takes form

$$\Delta g(x) = \frac{d^2 g(x_1)}{dx_1^2} g(x_2)g(x_3) + \frac{d^2 g(x_2)}{dx_2^2} g(x_1)g(x_3) + \frac{d^2 g(x_3)}{dx_3^2} g(x_1)g(x_2).$$

For a function presented in a Gaussian Galerkin basis $\{g_k(x)\}_{1\le k\le N_b}$, $x \in \mathbb{R}^3$, the Laplace operator takes the matrix form $A_g \in \mathbb{R}^{N_b \times N_b}$, with the entries

$$a_{km} = \langle \Delta g_k(x), g_m(x) \rangle, \quad k, m = 1, \dots N_b.$$

Let us consider the Laplace problem with the Dirichlet boundary conditions, posed in a volume box $[-b.b]^3$ on $n \times n \times n$ 3D Cartesian grid. The discrete 3D Laplace operator $\Delta_3 \in \mathbb{R}^{n^3 \times n^3}$ is represented by a tensor of rank 3,

$$\Delta_3 = \Delta_1^{(1)} \otimes I^{(2)} \otimes I^{(3)} + I^{(1)} \otimes \Delta_1^{(2)} \otimes I^{(3)} + I^{(1)} \otimes I^{(2)} \otimes \Delta_1^{(3)}, \tag{3.4}$$

where $\Delta_1^{(\ell)} = \Delta_1 \in \mathbb{R}^{n \times n}$, $\ell = 1, 2, 3$, and $I^{(\ell)} \in \mathbb{R}^{n \times n}$ is the identity matrix. Here the one-dimensional discrete Laplacian for the corresponding mode ℓ is

$$\Delta_1 = \frac{1}{h} \begin{bmatrix} 2 & -1 & \cdots & 0 & 1 \\ -1 & 2 & -1 & \cdots 0 & 0 \\ & \vdots & \ddots & \vdots & \vdots \\ 0 & \cdots & -1 & 2 & -1 \\ 0 & 0 & \cdots & -1 & 2 \end{bmatrix},$$

where h is the mesh-size of the uniform grid. The exact Galerkin matrix A_g is approximated using (3.2) and (3.4) as in [26], $A_g \approx A_G = \{\overline{a}_{km}\}$, $k, m = 1, \dots N_b$ with

$$\begin{aligned} \overline{a}_{km} &= \langle \Delta_1 G_k^{(1)}, G_m^{(1)} \rangle \langle G_k^{(2)}, G_m^{(2)} \rangle \langle G_k^{(3)}, G_m^{(3)} \rangle \\ &\quad + \langle G_k^{(1)}, G_m^{(1)} \rangle \langle \Delta_1 G_k^{(2)}, G_m^{(2)} \rangle \langle G_k^{(3)}, G_m^{(3)} \rangle \\ &\quad + \langle G_k^{(1)}, G_m^{(1)} \rangle \langle G_k^{(2)}, G_m^{(2)} \rangle \langle \Delta_1 G_k^{(3)}, G_m^{(3)} \rangle \\ &= \langle \Delta_3 \mathbf{G}_k, \mathbf{G}_m \rangle. \end{aligned} \tag{3.5}$$

The accuracy of this approximation is of order $\|a_{km} - \overline{a}_{km}\| = O(h^2)$.

3.3 3D Laplace operator in $O(\log n)$ complexity

The quantized $O(\log n)$ approximation for function related vectors and tensors was introduced in [31, 30]. It gives the opportunity to perform calculation of the multidimensional functions and operators in logarithmic complexity. Here, we use the quantized version of the Laplace operator introduced in [19]. For Δ_3 in (3.4), the rank-2 tensor train representation [38] is introduced in [19] as

$$\Delta_{3_T} = \begin{bmatrix} \Delta_1 & I \end{bmatrix} \otimes_b \begin{bmatrix} I & 0 \\ \Delta_1 & I \end{bmatrix} \otimes_b \begin{bmatrix} I \\ \Delta_1 \end{bmatrix}, \tag{3.6}$$

where the sign $\otimes_b$ denotes the matrix product of block core matrices, with blocks being multiplied by means of the tensor product. Suppose that $n = 2^L$, then the quantized representation of Δ_1, takes the form [19]

$$\Delta_{1_Q} = \begin{bmatrix} I & J & J \end{bmatrix} \otimes_b \begin{bmatrix} I & J & J \\ & J & \\ & & J \end{bmatrix}^{\otimes_b (L-2)} \otimes_b \begin{bmatrix} 2I - J - J \\ -J \\ -nJ \end{bmatrix}, \tag{3.7}$$

where L is equal to the number of the virtual dimensions in the quantized format, and

$$I = \begin{pmatrix} 1 & 0 \\ 0 & 1 \end{pmatrix}, \quad J = \begin{pmatrix} 0 & 1 \\ 0 & 0 \end{pmatrix}.$$

For the discretized representation (3.2) of the basis functions, the entries of the matrix $A_G = \{\overline{a}_{km}\}$, $k, m = 1, \dots N_b$ are calculated as

$$\overline{a}_{km} = \langle A_3 \mathbf{G}_k, \mathbf{G}_m \rangle \approx \langle \Delta_{3_Q} Q_k^{(1)} \otimes Q_k^{(2)} \otimes QG_k^{(3)}, Q_m^{(1)} \otimes Q_m^{(2)} \otimes QG_m^{(3)} \rangle, \tag{3.8}$$

where Δ_{3_Q} is obtained by substitution of QTT Laplace representation (3.7) into (3.6), and $Q_k^{(\ell)}$, $\ell = 1, 2, 3$, is the quantized representation of a vector $G_k^{(\ell)} \in \mathbb{R}^n$.

Numerical results demonstrate weak dependence of the calculation time on the size of the 3D Cartesian grid. Table 3.1 shows the approximation error for the Laplacian $err(A_G) = |A_{Molpro} - A_G|$ in Hartree-Fock calculations for water molecule, where A_{Molpro} is the result of analytical computations with the same Gaussian basis (from Molpro program [44]). Time is given for Matlab implementation. The line "RE" shows the Richardson approximation for the discrete Laplacian A_G computed on two adjacent grids.

3.4 $3D$ nuclear potential operator in 1D complexity

The nuclear potential operator describes the Coulomb interaction of the electrons with the nuclei,

$$V_c(x) = -\sum_{\nu=1}^{M} \frac{Z_\nu}{\|x - a_\nu\|}, \quad Z_\nu > 0, \;\; a_\nu \in \mathbb{R}^3, \tag{3.9}$$

where M is the number of nuclei, and a_ν, Z_ν, are the respective coordinates and charge numbers.

p	15	16	17	18	19	20
$n^3 = 2^{3p}$	32767^3	65535^3	131071^3	262143^3	524287^3	1048575^3
$err(A_G)$	0.0027	$6.8 \cdot 10^{-4}$	$1.7 \cdot 10^{-4}$	$4.2 \cdot 10^{-5}$	$1.0 \cdot 10^{-5}$	$2.6 \cdot 10^{-6}$
RE	-	$1.0 \cdot 10^{-5}$	$8.3 \cdot 10^{-8}$	$2.6 \cdot 10^{-9}$	$3.3 \cdot 10^{-10}$	0
time (sec)	12.8	17.4	25.7	42.6	77	135
Δa_{11}	49	12	3	0.7	0.19	0.0480
RE	-	0.3	0.0014	$3.3 \cdot 10^{-5}$	$3.3 \cdot 10^{-5}$	$3.3 \cdot 10^{-5}$

Table 3.1: 3D grid-based quantized tensor calculations for the water molecule (H_2O): accuracy and times versus 3D grid size for the Laplace Galerkin matrix $err(A_G)$ calculations using the discretized basis of $N_b = 41$ Cartesian Gaussians.

The tensor approximation of the Newton potential in a canonical tensor format with the rank-R_N introduced in [32, 6], is based on the application of the sinc approximation and the Laplace transform [15], and further piecewise constant discretization of resulting representation on the equidistant tensor grid $\omega_{\mathbf{3},n}$. Due to the tensor approximation $\mathbf{P}_{c,\nu}$ of the Newton kernel, we represent the nuclear potential for the molecule as a sum of M tensors placed in the coordinates of nuclei,

$$\mathbf{P}_c = \sum_{\nu=1}^{M} Z_\nu \mathbf{P}_{c,\nu}.$$

Note that for the grid-based representation of the Newton kernel, $\mathbf{P}_{c,\nu}$, the univariate grid size n can be noticeably smaller than the size of the grid used for the piecewise linear discretization for the Laplace operator. The entries of the respective part of the Fock matrix,

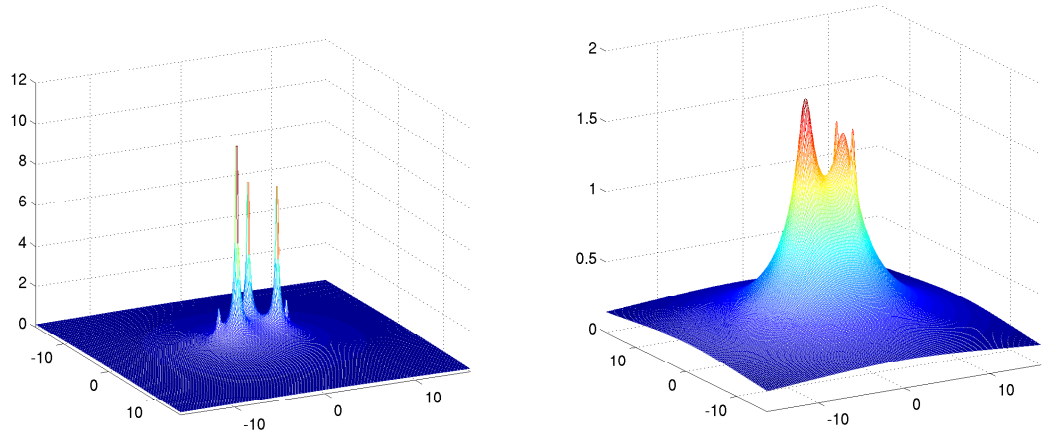

Figure 3.2: Nuclear potential $\mathbf{P}_c$ for the C_2H_5OH molecule, shown for the cross sections along x-axis, at the level $x = 0.0625$ au, and along y-axis, at level $y = 1.6$ au.

$V_G = \{\overline{v}_{km}\}$, are calculated (approximated) by projection of the $\mathbf{P}_c \in \mathbb{R}^{n^{\otimes 3}}$ to the discretized

basis functions $\{\overline{g}_k\}$,

$$\overline{v}_{km} = \int_{\mathbb{R}^3} V_c(x)\overline{g}_k(x)\overline{g}_m(x)dx \approx \langle \mathbf{G}_k \odot \mathbf{G}_m, \mathbf{P}_c \rangle, \quad 1 \le k, m \le N_b. \tag{3.10}$$

Figure 3.2 displays the nuclear potential for the molecule C_2H_5OH (ethanol) computed in a box $[-b, b]^3$, with $b = 16$ au. We show two cross-sections of the 3D function, at the level $x = 0.0625$ a.u., and at the permuted function at the level $y = -0.3125$ au. It is easy to notice from the left figure that three nonhydrogen atoms with the largest charges (two Carbon atoms with $Z = 6$ and one Oxygen atom with $Z = 8$) are placed on the plane $x = 0$. The right figure shows the location close to one of Hydrogen atoms.

The error $\varepsilon > 0$ arising due to the separable approximation of the nuclear potential is controlled by the rank parameter of the nuclear potential $R_P = rank(\mathbf{P}_c)$. Now letting $rank(\mathbf{G}_m) = R_m$ implies that each matrix element is to be computed with linear complexity in n, $O(R_k R_m R_P\, n)$. The almost exponential convergence of the rank approximation in R_P allows us the choice $R_P = O(|\log \varepsilon|)$.

3.5 Grid-based two-electron integrals

The incomplete Cholesky decomposition [13, 47] of the symmetric, positive definite matrix B,

$$B \approx LL^T, \quad L \in \mathbb{R}^{N_b^2 \times R_B}, \tag{3.11}$$

allows to optimize the Hartree-Fock calculations. Here we briefly recall the scheme introduced in [25, 27] for the 3D grid-based calculation of the two-electron integrals tensor in this factorized matrix form.

Given the discretized basis functions $\mathbf{G}_\mu$, $(\mu = 1, ..., N_b)$, we assume, without loss of generality, that $rank(\mathbf{G}_\mu) = 1$, i.e. $\mathbf{G}_\mu = G_\mu^{(1)} \otimes G_\mu^{(2)} \otimes G_\mu^{(3)} \in \mathbb{R}^{n\times n\times n}$. Let $\mathbf{G}^{(\ell)} = \left[\mathbf{G}_\mu^{(\ell)} \odot \mathbf{G}_\nu^{(\ell)}\right]_{1\le\mu,\nu\le N_b} \in \mathbb{R}^{n\times N_b\times N_b}$, $\ell = 1, 2, 3$, be the side tensor associated with a product-basis tensor $\mathbf{G} = [\mathbf{G}_{\mu\nu}]_{1\le\mu,\nu\le N_b}$, where $\mathbf{G}_{\mu\nu} := \mathbf{G}_\mu \odot \mathbf{G}_\nu$. Define the respective unfolding matrices

$$G^{(\ell)} = \mathrm{mat}(\mathbf{G}^{(\ell)}) \in \mathbb{R}^{n\times N_b^2}, \quad \ell = 1, 2, 3,$$

where $\mathbf{P}_\mathcal{N} \in \mathbb{R}^{n\times n\times n}$ is the rank-$R_\mathcal{N}$ canonical tensor approximating the Newton kernel in (2.8) [15, 6]. Then, the entries of the 4-th order tensor $\mathbf{B} = [b_{\mu\nu\kappa\lambda}]_{\mu\nu\kappa\lambda=1}^{N_b}$ can be evaluated by bilinear tensor operations as a sequence of $(n \log n)$ convolutions, and 1D Hadamard and scalar products [22, 25]

$$b_{\mu\nu\kappa\lambda} = \langle \mathbf{G}_{\mu\nu}, \mathbf{P}_\mathcal{N} * \mathbf{G}_{\kappa\lambda} \rangle_{n^{\otimes 3}}. \tag{3.12}$$

Though, here, the multidimensional integration is reduced to 1D complexity, the direct tensor-structured evaluation of (3.12) needs a storage size at least, $O(R_\mathcal{N} N_b^2 n)$, which can be problematic for large N_b of the order of several hundreds and large $n \approx 10^4$. In [25], a novel method for calculating the TEI is introduced, based on the factorized representation to the TEI matrix in a redundancy free modified product basis, which essentially decreases the number of convolution products in (3.12). The RHOSVD-type factorization [23] applied to the 3D tensor $\mathbf{G}$ allows us to represent it in a "squeezed" factorized form based on the

construction of dominating subspaces in the x-, y- and z- components in the product basis set.

Using the ε-truncated SVD-based left-orthogonal decomposition of $G^{(\ell)}$, $G^{(\ell)} \cong U^{(\ell)}V^{(\ell)^T}$, $\ell = 1, 2, 3$, with $n \times R_\ell$ and $N \times R_\ell$ matrices $U^{(\ell)}$ (orthogonal) and $V^{(\ell)}$, respectively, we obtain the so-called left and right redundancy-free (RF) basis sets, $U^{(\ell)}$, and $V^{(\ell)}$, respectively. The ranks of these decompositions can differ significantly for different space variables, depending on the molecular size and geometry. Numerical experiments show that the Frobenius error of these rank decompositions decays exponentially in the rank parameter, R_ℓ,

$$\|G^{(\ell)} - U^{(\ell)}V^{(\ell)^T}\|_F \leq Ce^{-\gamma_\ell R_\ell}, \quad \ell = 1, 2, 3.$$

The direct SVD of rectangular matrices $G^{(\ell)} \in \mathbb{R}^{n \times N_b^2}$ can be prohibitive even for the moderate size molecules ($n \geq 2^{13}$, $N_b \geq 200$). To get rid of this difficulty, we adapt the five-step algorithm [27] of the reduced computational and storage costs to compute the low-rank approximation $G^{(\ell)} \cong U^{(\ell)}V^{(\ell)^T}$ with the guaranteed tolerance $\varepsilon > 0$. It is based on the sequential application of the truncated Cholesky decomposition to the Gramm matrix $G^{(\ell)}G^{(\ell)^T}$, and the QR decomposition of the resulting factors. Given the rank-R_ℓ approximation $G^{(\ell)} \cong U^{(\ell)}V^{(\ell)^T}$ of the accuracy $\varepsilon > 0$, the redundancy-free factorized ε-approximation to the matrix B holds [25],

$$B \cong B_\varepsilon := \sum_{k=1}^{R_\mathcal{N}} \odot_{\ell=1}^{3} V^{(\ell)} M_k^{(\ell)} V^{(\ell)^T}, \tag{3.13}$$

where $V^{(\ell)}$ is the corresponding right RF basis, $\odot$ denotes the point-wise (Hadamard) product of matrices, and

$$M_k^{(\ell)} = U^{(\ell)^T}(P_k^{(\ell)} *_n U^{(\ell)}) \in \mathbb{R}^{R_\ell \times R_\ell}, \quad k = 1, ..., R_\mathcal{N}, \tag{3.14}$$

stands for the Galerkin convolution matrix on the left RF basis, $U^{(\ell)}$, $\ell = 1, 2, 3$, as described in the following algorithm.

Then, the TEI matrix is computed by the Cholesky decomposition algorithm, using (3.11) (as described in details in [25, 27]) where the separation rank $R_B \ll N_b^2$ is of order $O(N_b)$. Thus the tensor-structured approach provides calculation of the two-electron integrals in a "black-box way". Computation time depends on the size of the molecule (N_b), and on the required accuracy, which is defined both by the grid size n^3, and by the tolerance error ε. It is possible to optimize the rank-structured representation of the matrix$B$, by employing the QTT-structure in column vectors of L.

Precomputed tensors $\mathbf{G}_{\mu\nu}, \mathbf{H}_{\kappa\lambda}$, in view of (3.12), we have

$$J(D)_{\mu\nu} = \sum_{\kappa,\lambda=1}^{N_b} b_{\mu\nu,\kappa\lambda} D_{\kappa\lambda} = \sum_{\kappa,\lambda=1}^{N_b} \langle \mathbf{G}_{\mu\nu}, \mathbf{H}_{\kappa\lambda} \rangle D_{\kappa\lambda}. \tag{3.15}$$

Vectorizing matrices $\overline{J} = vec(J), \overline{D} = vec(D)$, we arrive at the simple matrix representation,

$$\overline{J} = B\overline{D} \approx L(L^T\overline{D}), \tag{3.16}$$

which can be easily evaluated taking into account the rank structure of B as well as the QTT-structure in vectors $\overline{D}$ and in the column vectors of L.

The straightforward calculation by (3.13) amounts to $O(R_B N_b^2)$ operations where R_B is the ε-rank of B. Our analysis indicates that imposing the QTT-structure of the matrix L may reduce this cost to $O(R_B N_{orb} N_b)$.

In tensor calculation of the exchange matrix $K(D)$ the summation is performed over permuted indices (2.10).

$$K(D)_{\mu\nu} = -\frac{1}{2}\sum_{\kappa,\lambda=1}^{N_b} b_{\mu\lambda,\nu\kappa} D_{\kappa\lambda} = -\frac{1}{2}\sum_{\kappa,\lambda=1}^{N_b} \langle \mathbf{G}_{\mu\lambda}, \mathbf{H}_{\nu\kappa} \rangle D_{\kappa\lambda}. \tag{3.17}$$

Introducing the permuted tensor $\widetilde{\mathbf{B}} = permute(\mathbf{B}, [2,3,1,4])$, and the respective accompanying matrix $\widetilde{B} = mat(\widetilde{\mathbf{B}})$, we then obtain

$$vec(K) = \overline{K} = \widetilde{B}\overline{D}. \tag{3.18}$$

The calculation by (3.18) amounts to $O(R_B N_b^3)$ operations. However, using the rank-N_{orb} decomposition of $D = 2CC^T$ allows to reduce the cost to $O(R_B N_{orb} N_b^2)$, by the representation,

$$K(D)_{\mu\nu} = -\sum_{i=1}^{N_{orb}} (\sum L_{\mu\lambda} C_{\lambda i})(\sum L_{\kappa\nu} C_{\kappa i})^T, \tag{3.19}$$

where $L_{\mu\nu} = reshape(L, [N_b, N_b, R_B])$ is the $N_b \times N_b \times R_B$-unfolding of the Cholesky factor L.

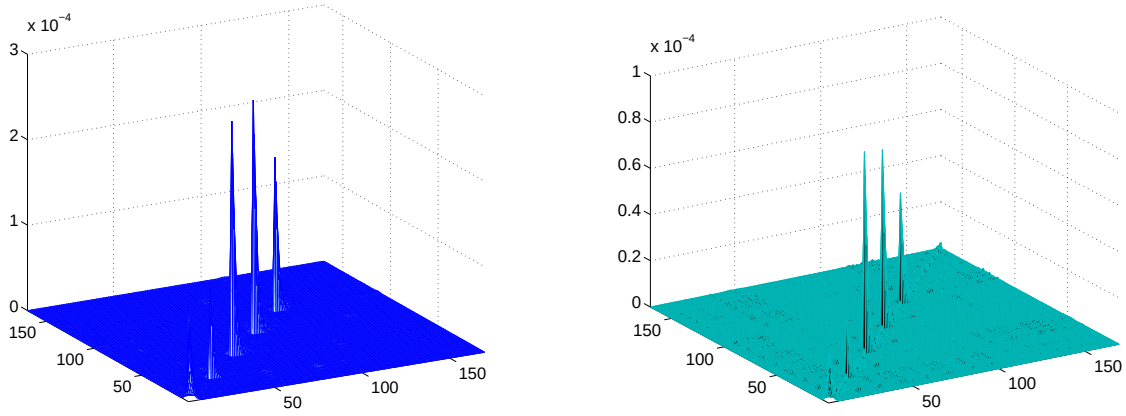

Figure 3.3: The quality of TEI calculations can be tested before the EVP, by using the coefficients for the density matrix from Molpro. Approximation accuracy for the Coulomb matrix of the Glycine molecule using TEI computed on the grid with $n^3 = 32768^3$ (left) and $n^3 = 65536^3$ (right).

3.6 Algorithm of the black-box HF solver

Our tensor-based HF solver operates in a black-box way: one should only set the coordinates and charges of nuclei, give the grid representation of the Galerkin basis and start the program.

For molecules, the charges Z_m and coordinates (x_m, y_m, z_m), $m = 1, \ldots, M$ of the nuclei in a molecule should be fixed. For extended systems one should define the coordinates and Galerkin basis of an "initiating atom", the interval between atoms, and the number of atoms in direction of each of space variables. At this work, for constructing the Galerkin basis we apply the rank-1 basis functions given as Gaussians with a table of coefficients for exponents, polynomial powers and shifts. The appropriate grid sizes should be chosen according to the required accuracy of calculations. As it was already noted, the grid-size n of the $n \times n \times n$ of 3D Cartesian grid can be chosen different for discretized calculation of the Laplacian, the nuclear potential operator, and TEI. Larger grids need more time, therefore, there is a playoff between the required accuracy and calculation time.

Given the coordinates of nuclei and the Galerkin basis, our black-box HF solver performs implicitly the following computation steps, as shown in Algorithm 1. For small and medium

Algorithm 1 Ab-initio black-box Hartree-Fock solver

Input: size b of the computational box, $[-b, b]^3$,
number M of nuclei in a molecular system,
charges Z_m and coordinates of nuclei (x_m, y_m, z_m), $m = 1, \ldots, M$,
size n of $n \times n \times n$ of 3D Cartesian grid,
discrete representation of basis functions (3.3) on tensor grid,
accuracy thresholds for calculating TEI and other integrals,
accuracy threshold $\varepsilon \geq 0$ to stop iteration,
integer $M_{opt} \geq 2$ for the DIIS scheme.
(1) Compute the nuclear energy shift E_{nuc}, by (2.12).
(2) Compute the Galerkin matrix of the core Hamiltonian, including
A_G for the Laplacian (3.8) and V_G for the nuclear potential operator (3.10).
(3) Compute mass matrix S for the given basis.
(4) Compute TEI matrix, in a form $B = LL^T$ by (3.13), (3.14).
(5) SCF iteration. For iteration $k = 1$ set matrices $J = 0$, $K = 0$.
Start SCF iteration.
Solve the EVP (2.5) with $F = 0.5 * A_G - V_G + J - K$,
(If $it \geq M_{opt}$, include the weights from DIIS update.)
Update J, K by computing (3.16) and (3.19).
Compute the ground state energy $E_{0,n,k}$ at current iteration k.
For iteration k, compute difference $w_i = |c_{i,k-1} - c_{i,k}|$, $i = 1, \ldots, N_{orb}$,
of the parts of the row vectors in FC, $c_i = \{a_j\}_{j=N_{orb}}^{N_b}$.
Compute the weights for DIIS scheme.
If $\|w_i\|_\infty \geq \varepsilon$, $i = 1, \ldots, N_{orb}$ continue iteration.
(6) (optionally) MP2 correction E_{MP2} by factorizations introduced in [27].
Output: Ground state energy $E_{0,n}$, set of occupied orbitals, etc.

size molecules the program works in one run from the first step to the end of SCF iteration,

using 3D Cartesian grids up to $n^3 = 131072^3$. Computation time usually equals to several minutes in Matlab. For larger molecules (amino acids) accurate calculations with the grid exceeding $n^3 = 65536^3$ need a separate run for TEI, requiring 2-3 hours of Matlab calculations. Time for TEI depends largely more on the number of basis functions, than on the size of the grid. The grid size is defined by the available storage of the computer: storage demand for the first step in TEI calculations (factorization of side matrices $\mathbf{G}^{(\ell)} \in \mathbb{R}^{n \times N_b^2}$, $\ell = 1, 2, 3$, see Appendix in [27]), equals to $O(3nN_b^2)$, while for the second step of TEI (Cholesky decomposition of matrix B) it is approximately $O(N_b^3)$.

4 Numerical simulations

Numerical simulations are performed in MATLAB on a 8 AMD Opteron Dual-Core / 2800 computer cluster. The molecule is considered in a computational box, $[-b, b]^3$, with $b = 20$ au (≈ 10.6 $\mathring{A}$). In TEI calculations we use the uniform mesh sizes up to finest level with $h = 2.5 \cdot 10^{-4}$, cooresponding to approximately $1.3 \cdot 10^{-4}$ $\mathring{A}$. For the core Hamiltonian finer grids are required, with the mesh size $h = 3.5 \cdot 10^{-5}$ au ($\sim 1.8 \cdot 10^{-5}$ $\mathring{A}$). These corresponds to 3D Cartesian grids with $n^3 = 65535^3$ and $n^3 = 1048576^3$ entries, correspondingly.

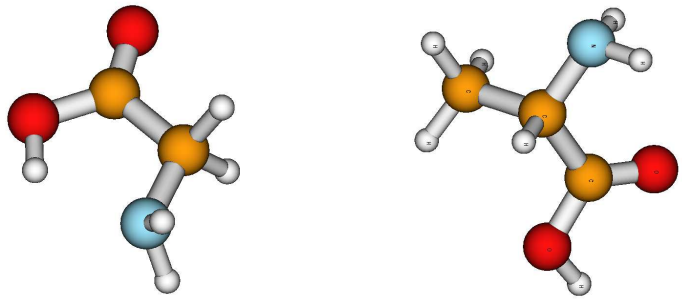

Figure 4.1: The largest molecules considered in this paper, amino acids glycine $C_2H_5NO_2$ (left) and alanine $C_3H_7NO_2$ (right). The ball-stick picture of molecules is generated by the MOLDEN program [41]).

4.1 Ab initio ground state energy calculations for compact molecules

In this section, we present calculations of the ground state energy for several compact molecules. For convenient comparison of the results with the Molpro program, the same Gaussian basis sets are used, represented on the grid, as discussed in §3.1.

Table 4.1 presents the error in ground state energy $er(E_0) = E_{0,n} - E_{0,Molpro}$ versus the mesh size of the grid for calculating TEI, h for glycine molecule. The error of grid-based calculations does not change beginning with the grid size 65535^3, remaining at the order of 10^{-4} hartree.

p	13	15	16	17
$n^3 = 2^{3p}$	8192^3	32767^3	65535^3	131072^3
h	0.0039	$9.7 \cdot 10^{-4}$	$4.9 \cdot 10^{-4}$	$2.5 \cdot 10^{-4}$
$E_{0,n}$	-282.8679	-282.8655	-282.8654	-282.8653
$er(E_0)$	0.0024	$3.5 \cdot 10^{-4}$	$2.2 \cdot 10^{-4}$	$2.2 \cdot 10^{-4}$

Table 4.1: Glycine, basis of 170 Gaussians (cc-pVDZ): error in ground state energy versus the mesh size h. Molpro result $E_{0,Molpro} = -282.8651$.

Figures 4.2–4.3 show convergence of the SCF iterations for glycine ($N_b = 170$) and alanine ($N_b = 211$) molecules, using the factorized representation of TEI computed on the grids with $n^3 = 131072^3$ and $n^3 = 32768^3$, respectively. Green line shows convergence of the residual, computed as the difference of the eigenvectors from two consequent iterations. Blue line presents the difference between the lowest eigenvector computed by the grid-based solver with the same eigenvalue from MOLPRO calculations, $\Delta\lambda_1 = |\lambda_{1,Molpro} - \lambda_{1,n}|$. Red line is the difference in ground state energy with the Molpro calculations when using the same basis functions. Note that the error of the grid-based calculations for these molecules does not change beginning from the grid size with $n = 32768$, remaining at the order of 10^{-4} hartree.

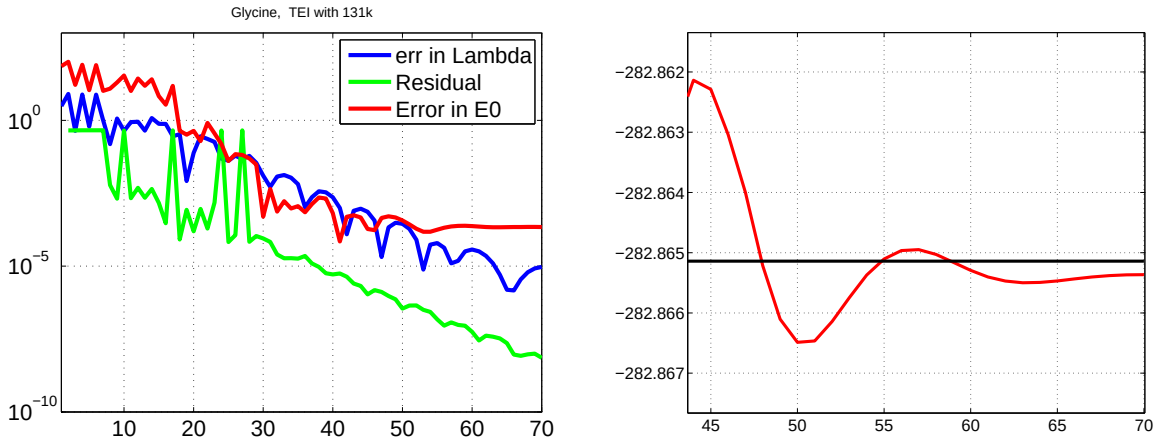

Figure 4.2: Left: SCF iterations history for the glycine molecule ($N_b = 170$), using TEI factorisation on the grid $n^{\otimes 3} = 131072^3$. Right: Calculations with $n = 65536$: $E_{0,n}$ (red) versus iteration step $(30+it)$, black line correspond to $E_{0,Molpro}$ for the same Gauusian basis.

Figure 4.4 shows the results for H_2O molecule, where the figure in the center shows the convergence of the ground state energy versus the iteration number, and the figure on the right displays the computed the grid based ground state energy vs $30 + k$ iterations. The black line shows the E_0 from Molpro for the same basis.

Figure 4.5 presents the last $30 + k$ iterations on convergence of the ground state energy. Red, green and blue lines correspond to grids $n^3 = 32768^3$, 65536^3 and 131072^3, correspondingly.

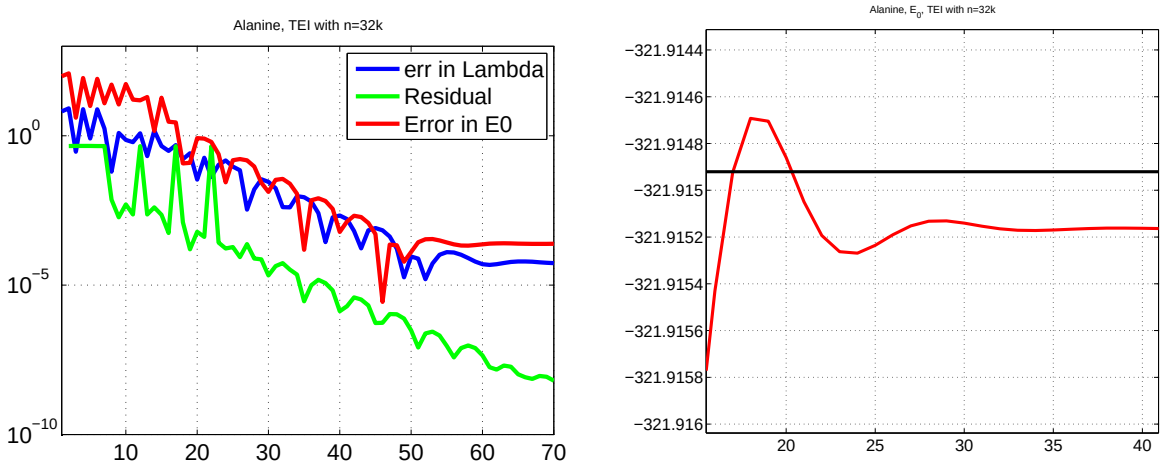

Figure 4.3: Left: SCF iteration for alanyne molecule ($N_b = 211$), with TEI computed on the grid $n^{\otimes 3} = 32768^3$. Right: the red line shows $E_{0,n}$ versus iteration step $(30 + it)$, black line correspond to $E_{0,Molpro}$ for the same basis cc-pVDZ of 211 Gaussians.

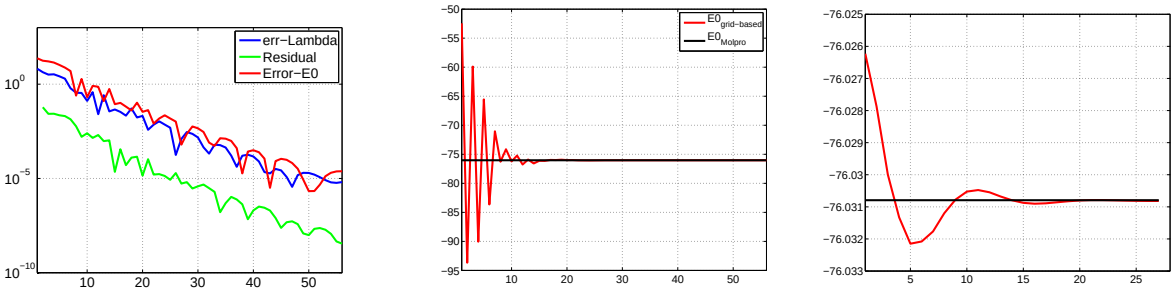

Figure 4.4: The H_2O molecule. Left: convergence for the residual (green), and the errors for the lowest eigenvalue (blue), and the ground state energy (red). Center: convergence of the ground state energy versus the iteration number. Right figure: computed E_0 vs $30 + k$ iterations. Black line is $E_{0,Molpro}$ from Molpro.

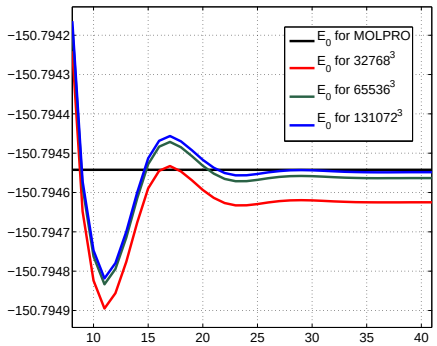

Figure 4.5: Left: molecule H_2O_2, convergence of grid-based $E_{0,n}$ after $30+k$ iterations. Black line shows the Molpro result for the same basis.

4.2 Black-box HF calculations for model extended systems

For modeling the extended systems, we construct an artificial crystall-like structure by using a sigle atom as an initiating block, and multiply translating it at equal intervals d_1, d_2, d_3, for every of three spacial directions, x, y, and z, respectively. Thus a 3D lattice of size $m_1 \times m_2 \times m_3$, is assembled, where m_1, m_2, m_3 are the number of atoms in the spatial directions x, y, and z.

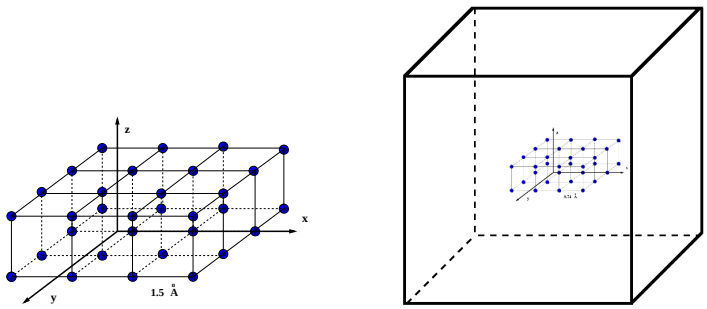

Figure 4.6: The periodic structure of the size $4.5 \times 4.5 \times 1.5$ $\overset{\circ}{A}^3$ in the computational box $[-b, b]^3$, with $b = 16$ au (~ 8.5 $\overset{\circ}{A}$) .

Several basis functions (at present stage, Gaussians) taken for a single atom as the "initialization basis" are duplicated for the lattice atoms, thus creating the basis set for the whole molecular system.

As a model problem we construct the artificial structures using the Hydrogen atoms, in a form of the 16×2, 8×4, and 8×8 slabs and a crystall-like structure of $4 \times 4 \times 2$ H atoms.

As the "initiating" building block a Hydrogen molecule H_2 is used with the distance between atoms equal to 1.5 $\overset{\circ}{A}$. Then for a network constructed as described above, one can start the black-box solver. For the Hydrogen-based lattice construction the ground state energy is computed "on-the-fly", calculations for TEI and Fock operator are done in one run. Figure 4.7 shows the slices of the nuclear potential calculated for the slab with $8 \times 8 \times 1$ Hydrogen atoms. The decay of the total nuclear potential is shown on the comparison of the planes corresponding to levels $z = 0$ and $z = 0.75$ au.

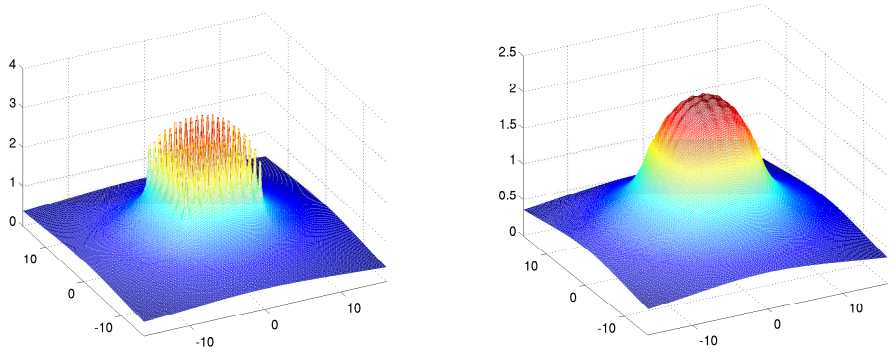

Figure 4.7: Decay of the nuclear potential for $8 \times 8 \times 1$ cluster of H atoms.

Figures 4.8 show the negative part of the spectra (each line standing for an eigenvalue) resulting from the HF calculations for the slabs with the sizes $16 \times 2 \times 1$ and $8 \times 4 \times 1$. It is easy to notice that the spectra for slabs $16 \times 2 \times 1$ and $8 \times 4 \times 1$ are similar.

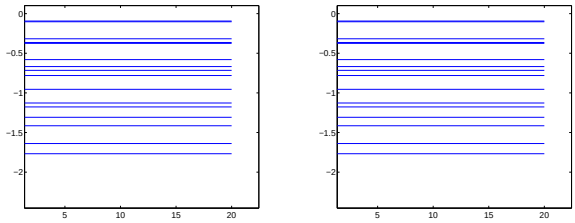

Figure 4.8: The negative part of spectra λ_i for the model systems of the size 16×2 and 8×4.

5 Conclusions

We present the 3D grid-based black-box solver for the Hartree-Fock equation, which is compatible in performance with established quantum chemical packages based on analytical integration in $\mathbb{R}^3$. The numerical results show successful application of this solver in *ab initio* electronic structure calculations for large compact molecules and model extended systems.

Tensor Hartree Fock calculations do not have special requirements on the positions of nuclei on the 3D grid, the nuclei in the investigated molecular systems may have an arbitrary position in (x, y, z)-coordinates in the computational box. There is no need of the additional precomputed data. Due to the tensor-structured methods, complexity of the computations on $n \times n \times n$ 3D Cartesian grids is of the order of $O(n \log n)$ for the TEI convolutions, and of $O(n)$ to $O(\log n)$ in calculation of the 3D Laplace and the nucler potential operators.

Our approach gives the opportunity to compute TEI tensor and the Fock operator "on the fly", in the case of multiply varying and rather general basis sets specified by their grid representation. Due to affording an easy change of bases, this solver can be applicable in the potential energy surface calculations in molecular dynamics,

The tensor-structured black-box HF solver can be further used for the numerical solution of the Hartree-Fock equation for the arbitrary molecular geometry or extended structures in a *black-box* way: just insert the coordinates of atoms and the discretized basis and start the program.

Currently, it is successfully applied to investigate the stretched systems of atomic chains and crystall-like 2D and 3D structures of Hydrogen atoms. Thus, the tensor numerical methods in electronic structure calculations, developed initially for single compact molecules, can be extended to periodic and quasi-periodic systems.

6 Appendix A. Electronic Schrödinger equation

The Hartree-Fock model originates from the electronic Schrödinger equation,

$$\mathcal{H}\Psi = E\Psi, \tag{6.1}$$

with the Hamiltonian

$$\mathcal{H}_e = -\frac{1}{2}\sum_{i=1}^{N}\Delta_i + \sum_{i=1}^{N}\sum_{A=1}^{M}\frac{Z_A}{x_i - x_A} + \sum_{\substack{i,j=1\\ i\neq j}}^{N}\frac{1}{|x_i - x_j|}, \quad x_A \in \mathbb{N}, \quad x_i, x_j \in \mathbb{R}^3, \tag{6.2}$$

which describes the energy of a molecular system in the framework of the so-called Born-Oppenheimer approximation, implying a system with clapped nuclei. Since the nuclei are much heavier than electrons, and their motion is much slower, the nuclei and electronic parts of the energy can be considered separately. Thus, the electronic Schrödinger equation specifies the energy of a molecular system at a fixed nucler geometry. The Hamiltonian (6.2) includes the kinetic energy of electrons, the potential energy of the interaction between nuclei and electrons, and the electron correlation energy. Here M is the number of nuclei, Z_A are nuclei charges and N is the number of electrons in a molecule. The electronic Schrödinger equation is a multidimensional problem in $\mathbb{R}^{3N}$, and it is unsolvable except for the Hydrogen or Hydrogen-like atoms.

The Hartree-Fock equation, which can be solved numerically since it is a $3D$ problem in space variables, is obtained as a result of the minimization of the energy functional for the electronic Schrödinger equation [43, 12]. The underlying condition for the wavefunction is, that it should be a single Slater determinant containing the products of electronic orbitals. For fermions the wavefunction Ψ should be antisymmetric, therefore it is parametrized using a Slater determinant approximation,

$$\Psi = \frac{1}{N!}\begin{vmatrix} \varphi_1(x_1) & \varphi_2(x_1) & \dots & \varphi_N(x_1) \\ \varphi_1(x_2) & \varphi_2(x_2) & \dots & \varphi_N(x_2) \\ \dots & \dots & \dots & \dots \\ \varphi_1(x_N) & \varphi_2(x_N) & \dots & \varphi_N(x_N) \end{vmatrix},$$

where $\varphi_i(x_j)$ are the one-electron wavefunctions, $i, j = 1, \dots N$. We refer to literature on electronic structure calculations for the derivation of the Hartree-Fock equation [43, 12].

7 Appendix B. Basic tensor formats and operations

A tensor of order d, a multidimensional array given by a d-tuple index set,

$$\mathbf{A} = [a_{i_1,\dots,i_d}] \in \mathbb{R}^{n_1\times\dots\times n_d},$$

is an element of a linear vector space equipped with the Euclidean scalar product. A tensor with equal sizes $n_\ell = n$, $\ell = 1, \dots d$, is called an $n^{\otimes d}$ tensor. The required storage size scales exponentially in the dimension, n^d, (the so-called "curse of dimensionality").

To get rid of exponential scaling in the dimension, one can apply the rank-structured representations of multidimensional tensors. The rank-1 canonical tensor,

$$\mathbf{A} = u^{(1)} \otimes ... \otimes u^{(d)} \in \mathbb{R}^{n_1 \times ... \times n_d} \quad \text{with entries} \quad u_{i_1,...i_d} = u^{(1)}_{i_1} \cdots u^{(d)}_{i_d},$$

requires only dn numbers to store it. A tensor in the R-term canonical format is defined as

$$\mathbf{A} = \sum_{k=1}^{R} c_k u^{(1)}_k \otimes \ldots \otimes u^{(d)}_k, \quad c_k \in \mathbb{R}, \tag{7.1}$$

where $u^{(\ell)}_k$ are normalized vectors, and R is called the canonical rank of a tensor. The tensor in the rank-$\mathbf{r}$ Tucker format, with the rank $\mathbf{r} = (r_1, ..., r_d)$, is defined as

$$\mathbf{A} = \sum\nolimits_{\nu_1=1}^{r_1} \cdots \sum\nolimits_{\nu_d=1}^{r_d} \beta_{\nu_1,...,\nu_d}\, v^{(1)}_{\nu_1} \otimes \ldots \otimes v^{(d)}_{\nu_d}, \quad \ell = 1, \ldots, d$$

with the set of orthonormal vectors $v^{(\ell)}_{\nu_\ell} \in \mathbb{R}^{n_\ell}$, and the core tensor $\boldsymbol{\beta} = [\beta_{\nu_1,...,\nu_d}]$. For function related tensors $r_\ell \ll n$, [32]. Rank-structured tensor representation provides fast multi-linear algebra with linear complexity scaling in the dimension d. For given canonical tensors $\mathbf{A}_1$, $\mathbf{A}_2$, the Euclidean scalar product can be computed by

$$\langle \mathbf{A}_1, \mathbf{A}_2 \rangle := \sum_{k=1}^{R_1} \sum_{m=1}^{R_2} c_k b_m \prod_{\ell=1}^{d} \left\langle u^{(\ell)}_k, v^{(\ell)}_m \right\rangle,$$

at the expense $O(dnR_1R_2)$. The Hadamard product of tensors $\mathbf{A}_1, \mathbf{A}_2$ given in the canonical format (7.1) is calculated in $O(dnR_1R_2)$ operations by

$$\mathbf{A}_1 \odot \mathbf{A}_2 := \sum_{k=1}^{R_1} \sum_{m=1}^{R_2} c_k b_m \left(u^{(1)}_k \odot v^{(1)}_m \right) \otimes \ldots \otimes \left(u^{(d)}_k \odot v^{(d)}_m \right).$$

In electronic structure calculations, the 3D convolution transform with the Newton kernel, $\frac{1}{\|x-y\|}$, is the most computationally expensive operation. The tensor method to compute convolution over large $n \times n \times n$ Cartesian grids in $O(n \log n)$ complexity was introduced in [29]. Given canonical tensors $\mathbf{A}_1$, $\mathbf{A}_2$ in a form (7.1), their convolution product is represented by the sum of tensor products of $1D$ convolutions,

$$\mathbf{A}_1 * \mathbf{A}_2 = \sum_{k=1}^{R_1} \sum_{m=1}^{R_2} c_k b_m \left(u^{(1)}_k * v^{(1)}_m \right) \otimes \left(u^{(2)}_k * v^{(2)}_m \right) \otimes \left(u^{(3)}_k * v^{(3)}_m \right), \tag{7.2}$$

where $u^{(\ell)}_k * v^{(\ell)}_m$ is the convolution product of n-vectors. The cost of tensor convolution in both storage and time is estimated by $O(R_1R_2n \log n)$. It considerably outperforms the conventional 3D FFT-based algorithm of complexity $O(n^3 \log n)$ [23].

In tensor-structured numerical methods the calculation of the $3D$ convolution integrals is replaced by a sequence of $1D$ scalar and Hadamard products, and $1D$ convolution transforms [23, 22]. However, the rank-structured operations lead to increasing of tensor ranks which

can be reduced by the canonical-to-Tucker and Tucker-to-canonical algorithms introduced in [33, 23, 22].

For problems in higher dimensions, the rank-structured tensor representation of functions in tensor train (TT) [38] format. In physics it was introduced earlier as the matrix-product states (MPS) format [46]. An entry of a d-dimensional tensor in this format is given by

$$a(i_1, i_2, \ldots, i_d) = A^{(1)}_{i_1} A^{(2)}_{i_2} \ldots A^{(d)}_{i_d}, \tag{7.3}$$

where each $A^{(k)}_{i_k} = G^{(k)}(\alpha_{k-1}, i_k, \alpha_k)$ is $r_{k-1} \times r_k$ matrix depending on i_k with the convention $r_0 = r_d = 1$. Storage needs for $n^{\otimes d}$ TT tensor is to $O(dr^2 n)$, $r = \max r_k$. The algebraic operations on TT tensors can be implemented with linear complexity scaling in n and d.

The $O(d \log n)$-quantics approximation method for vectors have been introduced in 2009 by Boris Khoromskij, see [30, 31]. It provides a compressed quantized (QTT) representation of function-related vectors and and rank-structured tensors, with logarithmic scaling of storage. The QTT representation of functional vectors of size $n = 2^L$ needs only

$$2 \cdot L \cdot k^2 \ll 2^L$$

numbers, where k is the QTT-rank, thus providing logarithmic reduction of storage and computational complexity.

In [30, 31] it is proven that the rank k in the QTT approximation is a small constant for a wide class of discretized functions: $k = 1$ for complex exponents, $k = 2$ for trigonometric functions and for Chebyshev polynomial on Chebyshev-Gauss-Lobatto grid, $k \leq m + 1$ for polynomials of degree m, k is a small constant for wavelet basis functions, etc.

The QTT approximation method allows to represent a class of matrices in low QTT rank format [19], and enables the multidimensional FFT and convolution transforms with logarithmic complexity scaling, $O(\log n)$, [7, 20].

Acknowledgements. The author is grateful to PD DrSci. Boris Khoromskij for fruitful collaboration in our joint work on the tensor methods for the Hartree-Fock problem. The author is appreciative to Dr. Heinz-Juergen Flad (TU München) for stimulating discussions and to Prof. Dr. Reinhold Schneider (TU Berlin) for the support of the tensor-based Hartree-Fock project. The author is appreciative to PD Dr. Dirk Andrae (FU Berlin) for providing the Molpro data.

References

[1] R. Ahlrichs, M. Bär, M. Häser, H. Horn, Ch.Kölmel. *Electronic structure calcualtions on workstation computers: The program system turbomole.* Chemical Physics Letters, 162(3), 1989, 165-169.

[2] J. Almlöf. *Direct methods in electronic structure theory.* In D. R. Yarkony: Modern Electronic Structure Theory. vol II, World Scientific, Singapore, 1995 pp. 110-151.

[3] J. Ballani, L. Grasedyck. *A Projection Method to Solve Linear Systems in Tensor Format.* Num. Lin. Alg. Appl. 1, (2013), 27-43.

[4] M. Bachmayr. *Adaptive low-rank wavelet methods and applications to two-electron Schrdinger equations.* PhD Dissertation, RWTH Aachen, 2012.

[5] M. Barrault, E. Cancés, W. Hager and C. Le Bris. *Multilevel domain decomposition for electronic structure calculations.* J. Comput. Phys. **222**, 2007, 86-109.

[6] C. Bertoglio, and B.N. Khoromskij. *Low-rank quadrature-based tensor approximation of the Galerkin projected Newton/Yukawa kernels.* Comp. Phys. Communications, v. 183(4), 904-912 (2012).

[7] S.V. Dolgov, B.N. Khoromskij, and D. Savostianov. *Superfast Fourier transform using QTT approximation.* J. Fourier Anal. Appl., 2012, vol.18, 5, 915-953.

[8] W. Hackbusch. *Tensor spaces and numerical tensor calculus.* Springer, 2012.

[9] W. Hackbusch and B.N. Khoromskij. *Low-rank Kronecker product approximation to multi-dimensional nonlocal operators. Part I. Separable approximation of multi-variate functions;* Computing **76** (2006), 177-202.

[10] W. Hackbusch, B.N. Khoromskij, S. Sauter, and E. Tyrtyshnikov. *Use of tensor formats in elliptic eigenvalue problems.* Numer. Lin. Alg. Appl., v. 19(1), 2012, 133-151.

[11] R.J. Harrison, G.I. Fann, T. Yanai, Z. Gan, and G. Beylkin. *Multiresolution quantum chemistry: Basic theory and initial applications.* J. of Chemical Physics, 121 (23): 11587-11598, 2004.

[12] T. Helgaker, P. Jørgensen, and J. Olsen. *Molecular Electronic-Structure Theory.* Wiley, New York, 1999.

[13] N. Higham. *Analysis of the Cholesky decomposition of a semi-definite matrix.* In M.G. Cox and S.J. Hammarling, eds. Reliable Numerical Computations, p. 161-185, Oxford University Press, Oxford, 1990.

[14] I.P. Gavrilyuk, W. Hackbusch and B.N. Khoromskij. *Data-Sparse Approximation to a Class of Operator-Valued Functions.* Math. Comp. 74 (2005), 681-708.

[15] I.P. Gavrilyuk, W. Hackbusch and B.N. Khoromskij. *Hierarchical Tensor-Product Approximation to the Inverse and Related Operators in High-Dimensional Elliptic Problems.* Computing 74 (2005), 131-157.

[16] L. Grasedyck, D. Kressner and C. Tobler. *A literature survey of low-rank tensor approximation techniques.* arXiv:1302.7121v1, 2013.

[17] M. Griebel and J. Hamaekers. Tensor Product Multiscale Many-Particle Spaces with Finite-Order Weights for the Electronic Schrödinger Equation. Zeitschrift für Physikalische Chemie, 224 (2010), 527-543.

[18] R.J. Harrison, G.I. Fann, T. Yanai, Z. Gan and G. Beylkin, *Multiresolution quantum chemistry: Basic theory and initial applications.* J. Chem. Phys. 121, 11587–11598, 2004.

[19] V. Kazeev, and B.N. Khoromskij. *Explicit low-rank QTT representation of Laplace operator and its inverse.* SIAM Journal on Matrix Anal. and Appl., 33(3), 2012, 742-758.

[20] V. Kazeev, B.N. Khoromskij, and E.E. Tyrtyshnikov. *Multilevel Toeplitz matrices generated by QTT vectors and convolution with logarithmic complexity.* Preprint 36/2011, MPI MiS, Leipzig 2011, (SISC, to appear).

[21] V. Khoromskaia. *Computation of the Hartree-Fock Exchange in the Tensor-structured Format.* Comp. Meth. App. Math., 10(2) (2010) 204–218.

[22] V. Khoromskaia. *Numerical Solution of the Hartree-Fock Equation by Multilevel Tensor-structured methods.* Dissertation, TU Berlin, 2010. http://opus.kobv.de/tuberlin/volltexte/2011/2948/

[23] B.N. Khoromskij and V. Khoromskaia. *Multigrid Tensor Approximation of Function Related Arrays.* SIAM J. on Sci. Comp., **31**(4), 3002-3026, 2009.

[24] B.N. Khoromskij, V. Khoromskaia, and H.-J. Flad. *Numerical Solution of the Hartree-Fock Equation in Multilevel Tensor-structured Format.* SIAM J. Sci. Comp., **33**(1), 45-65, 2011.

[25] V. Khoromskaia, B.N. Khoromskij, and R. Schneider. *Tensor-structured factorized calculation of two-electron integrals in a general basis.* SIAM J Sci. Comp., **35**(2), A987-A1010 2013.

[26] V. Khoromskaia, D. Andrae, and B.N. Khoromskij. *Fast and accurate 3D tensor calculation of the Fock operator in a general basis.* Comp. Phys. Communications, 183 (2012) 2392-2404.

[27] V. Khoromskaia and B.N. Khoromskij. *Møller-Plesset (MP2) Energy Correction Using Tensor Factorizations of the Grid-based Two-electron Integrals.* Comp. Phys. Communications, DOI:10.1016/j.cpc.2013.08.004, 2013.

[28] B.N. Khoromskij. *Tensors-structured Numerical Methods in Scientific Computing: Survey on Recent Advances.* Chemometr. Intell. Lab. Syst. 110 (2012), 1-19.

[29] B.N. Khoromskij. *Fast and Accurate Tensor Approximation of a Multivariate Convolution with Linear Scaling in Dimension.* J. of Comp. Appl. Math., **234** (2010) 3122-3139.

[30] B.N. Khoromskij. *$O(d \log N)$-Quantics Approximation of N-d Tensors in High-Dimensional Numerical Modeling.* Preprint MPI MIS 55/2009, 2009.

[31] B.N. Khoromskij. *$O(d \log N)$-Quantics Approximation of N-d Tensors in High-Dimensional Numerical Modeling.* J. Constr. Approx., v.34(2), 2011, 257-289.

[32] B.N. Khoromskij, *Structured Rank-$(r_1, ..., r_d)$ Decomposition of Function-related Tensors in $\mathbb{R}^d$.* Comp. Meth. in Applied Math., **6** (2006), 2, 194-220.

[33] B. N. Khoromskij and V. Khoromskaia, *Low Rank Tucker Tensor Approximation to the Classical Potentials.* Central European J. of Math., **5**(3) 2007, 1-28.

[34] B.N. Khoromskij, and I. Oseledets. *DMRG+QTT approach to the computation of ground state for the molecular Schrödinger operator.* Preprint 68/2010, MPI MiS, Leipzig 2010.

[35] T.G. Kolda and B.W. Bader. *Tensor Decompositions and Applications. SIAM Review*, **51/3**, 2009 455-500.

[36] D. Kressner and C. Tobler. *Preconditioned low-rank methods for high-dimensional elliptic PDE eigenvalue problems.* Cpmutational Methods in Applied Mathematics, 2011, 11(3):363-381.

[37] G. I. Marchuk and V. V. Shaidurov. *Difference methods and their extrapolations.* Applications of Mathematics, New York: Springer, 1983.

[38] I.V. Oseledets, and E.E. Tyrtyshnikov, *Breaking the Curse of Dimensionality, or How to Use SVD in Many Dimensions.* SIAM J. Sci. Comp., 31 (2009), 3744-3759.

[39] P. Pulay, *Improved SCF convergence acceleration.* J. Comput. Chem. **3**, 556-560 (1982).

[40] D. V. Savostianov. Fast revealing of mode ranks of tensor in canonical form. Numer. Math. Theor. Meth. Appl. v.2 No.4 2009 pp439-444.

[41] G. Schaftenaar and J.H. Noordik. Molden: a pre- and post-processing program for molecular and electronic structures. J. Comput.-Aided Mol. Design, 14 (2000) 123-134.

[42] D. Sundholm, P. Pyykkö and L. Laaksonen. *Two-dimensional Fully Numerical Molecular Calculations. X. Hartree-Fock Results for He_2, Li_12, Be_2, HF, OH^-, N_2, CO, BF, NO^+, and CN^-.* Mol. Phys. 56 (1985) 1411-1418.

[43] A. Szabo ans N. Ostrlund. *Modern Quantum Chemistry.* Dover Publication, New York, 1996.

[44] H.-J. Werner, P.J. Knowles, et al. MOLPRO, Version 2002.10, A Package of Ab Initio Programs for Electronic Structure Calculations.

[45] H.-J. Werner, P.J. Knowles, G. Knozia, F. R. Manby and M. Schuetz. *Molpro: a general-purpose quantum chemistry program package.* WIREs Comput Mol Sci 2012, 2:242-253. doi:10.1002/wcms.82

[46] S.R. White. *Density-matrix algorithms for quantum renormalization groups.* Phys. Rev. B, v. 48(14), 1993, 10345-10356.

[47] S. Wilson. *Universal basis sets and Cholesky decomposition of the two-electron integral matrix.* Comput. Phys. Commun., 58:71-81, 1990.

[48] H. Yserentant. *Sparse grid spaces for the numerical solution of the electronic Schrödinger equation.* Numer. Math. 101 (2005), 381-389.

[49] H. Yserentant. *Regularity and Approximability of Electronic Wave Functions.* Lecture Notes in Mathematics series, Springer-Verlag, 2010.